4th QUARTER
No. 4 OCTOBER

Fire Technology, 37, 297–315, 2001

Non-Intrusive Measurements in Fire Sprinkler Sprays

John E Widmann, Building and Fire Research Laboratory, National Institute of Standards and Technology, Gaithersburg, Maryland 20899-8663, USA; john.widmann@nist.gov

David T. Sheppard,[1] Large Scale Fire Research, Underwriters Laboratories, Northbrook, IL 60062-2096, USA

Richard M. Lueptow, Department of Mechanical Engineering, Northwestern University, Evanston, IL 60208-3111, USA

Abstract. The results of phase Doppler interferometry (PDI) and particle image velocimetry (PIV) measurements to characterize the water sprays produced by fire sprinklers are presented. The large size of the water drops produced by fire sprinklers, and the relatively large coverage area of the spray, present significant challenges when attempting to characterize these sprays. These difficulties are especially relevant when using PDI because large drops and large coverage areas may result in attenuation of the transmitting laser beams. For the fire sprinkler investigated, it **was** determined that attenuation of the laser beam resulted in over-counting of drops due to burst splitting, a situation in which the Doppler signals from single drops are misinterpreted as being due to multiple drops. This effect was minimized by carefully choosing the operating conditions **of** the PDI processing electronics. PIV measurements provide velocity profiles that can be used as input for fire dynamics simulations to predict the effect of sprinkler sprays on fires. The results from the PIV measurements show good agreement with the velocity measurements obtained from PDI in the core of the spray, but poorer agreement along the sprinkler axis. The discrepancy was attributed to recirculation zones present in the experimental facility and possible biasing of the PIV measurements towards the larger drops.

Key words: fire sprinklers, drop size, drop velocity, **phase** Doppler interferometry, particle image velocimetry, sprinkler **sprays**

Intro

The basic function of a fire sprinkler is to extinguish or control an accidental fire, and the effectiveness of the sprinkler at controlling a fire is governed by the spray characteristics (e.g., spatial distributions of drop size, drop velocity, mass **flux).** For example, large drops can penetrate **a** rising fire plume to reach the fire source and wet combustible materials adjacent to the fire, whereas smaller drops may be entrained in the buoyant plume and carried away from the fire. Furthermore, the evaporating smaller drops have a cooling effect on the hot gases, and in some cases have been observed to prevent or delay the activation of additional fire sprinklers. It is therefore important that the spray characteristics of fire sprinklers be understood **if** the interaction of the spray and the fire

is to be understood and predicted. The reader is referred to the recent review by Grant *et al.* [1] for a thorough discussion of fire suppression by water sprays.

The rapid increase in computer technology has permitted more sophisticated modeling of the dynamics of fires. In particular, it is now possible to include the effects of water sprays on the fire spread. For example, the Fire Dynamics Simulator (FDS) developed at the National Institute of Standards and Technology (NIST) is used to predict large scale fire phenomena [2, 3] in a variety of fire scenarios. However, to include the effect of fire sprinklers on the fire dynamics it is necessary to provide characteristics of the water spray produced by the sprinklers. This information is generally unknown, and must be experimentally determined.

Previous studies characterizing fire sprinkler sprays have utilized photographic techniques [4–7] and a laser-light shadowing method [8–11]. The photographic methods included illuminating the drops using strobe lighting and pulsed lasers, and using still photographs and video cameras for image capture. The laser-light shadowing technique utilized a modified commercially available instrument intended for cloud drop measurements. The drops were sized by determining the number of pixels shadowed as the drops passed through a visible laser-light sheet illuminating a linear photodiode array. The (one-dimensional) drop velocity was also determined by the length of time the pixels were shadowed.

Sheppard *et al.* [12] demonstrated that particle image velocimetry (PIV) can be used to measure mean drop velocities in the sprays produced by residential fire sprinklers. Unfortunately, the PIV technique does not provide information on the drop size distributions or size-velocity correlations. Gandhi and Steppan [13] presented phase Doppler interferometry (PDI) measurements in industrial fire sprinkler sprays. They compared their volume **flux** measurements with pan test measurements, in which the spray was collected in pans for a known period of time, resulting in an independent volume flux measurement. They reported that the comparison was poor when the gauge pressure at the sprinkler head was 48.3 kPa (7 psig), but considerably better when the gauge pressure at the sprinkler was 153.1 kPa (22.2 **psig).** The correlation coefficients were 0.5259 and 0.8912 for the former and latter cases, respectively. Presumably, the increase in pressure resulted in significant changes in the spray characteristics, likely shifting the size distributions towards the smaller drops. They also reported a correlation coefficient of 0.9993 when PDI volume flux measurements were compared with pan test measurements for a water mist nozzle. Size and velocity distributions were not presented; however, a plot of drop diameter versus time suggests that the data correspond to a bimodal size distribution. The authors did not report the uncertainty in the measurements, but the good agreement between the PDI volume flux measurements and the pan test measurements (for the sprinkler at 153.1 kPa and the water mist nozzle) suggested that PDI may be a promising technique for characterizing fire sprinkler sprays.

Following the initial work of Gandhi and Steppan, Widmann [14] reported the results of a feasibility study to assess the accuracy of PDI measurements in water sprays produced by residential fire sprinklers. **A** single fire sprinkler was characterized, and the uncertainty in the measurements estimated. The results of that study indicate that accurate size and velocity measurements can be obtained in residential fire sprinkler sprays using PDI. For example, the uncertainties* in the arithmetic mean diameter and volume

mean diameter were reported to be 6.4% and 4.1%, respectively. Mean velocity measurements were reported with uncertainties of 6.9% (axial velocity) and 8.4% (radial velocity). Widmann [17] later compared the characteristics of four residential fire sprinklers and explored the effect of pressure on drop size.

This paper presents a discussion of the two non-intrusive diagnostic techniques that have recently been shown to be effective in characterizing the water sprays produced by fire sprinklers. Experimental data obtained at Underwriters Laboratories (UL) and NIST are presented, and the strengths and weaknesses of the two methods are discussed. Velocity measurements obtained with the two approaches are compared, and the sources of measurement uncertainty discussed.

Particle Image Velocimetry (PIV)

The PIV measurements presented in this paper were obtained in the sprinkler facility at Underwriters Laboratories in Northbrook, IL. The facility consists of an elevated circular traverse 3.7 m in diameter that can be rotated along the central axis. The sprinkler is located on the axis of the circular traverse, which permits the sprinkler to be rotated relative to the PIV optics. Thus, planar images can be obtained corresponding to different angular coordinates of the sprinkler without having to move and realign the PIV optical system. Using this system, the angular resolution of the measurements is estimated to be within 1°. A 3 m horizontal branch line is located beneath, and centered on the central axis of, the circular traverse. The sprinkler to be studied is attached to the branch line, which provides the water to the sprinkler. The branch line is mounted such that there is 4 m of clearance to the floor. Additional piping can be introduced to the branch line to extend the length if desired. The water to the sprinkler is supplied by one of three pumps, providing nominal flow rates up to 0.038 $m^3\ s^{-1}$ (600 gpm).

Figure 1 shows a schematic diagram illustrating the PIV technique. The mean velocity of the water drops is determined by obtaining two images in rapid succession. The displacement of the drops from the first image to the second is determined using a two-dimensional cross-correlation algorithm, and the velocity components in the plane of the light sheet are obtained from the displacement and the time delay between laser pulses. A solid-state Nd:YAG pulsed laser was used as the illumination source for the PIV measurements. The pulse duration of the laser was approximately 6–7 ns, and the time between laser pulses was 66 μs. The average energy output was nominally 25 mJ. The CCD camera used for image capture contained a 1000 × 1000 pixel array. The imaged area was 295 mm × 295 mm resulting in an image resolution of 295 μm per pixel. Additional details of the experimental arrangement are presented in [12].

The experimental PIV data presented herein correspond to a Grinnel[3] Model FR-1 fire sprinkler, and were obtained at the Underwriters Laboratories facility described above. The sprinkler has a K-factor of $1.33 \times 10^{-4}\ m^3\ s^{-1}\ kPa^{-0.5}$ (5.5 gal min^{-1} $psig^{-0.5}$). The pressure at the sprinkler head was maintained at 51.7 kPa ± 6.9 kPa (7.5 psig ± 1.0 psig), resulting in a flow rate through the sprinkler of $9.47 \times 10^{-4}\ m^3\ s^{-1} \pm 0.63 \times 10^{-4}\ m^3\ s^{-1}$ (15 gpm ± 1 gpm).

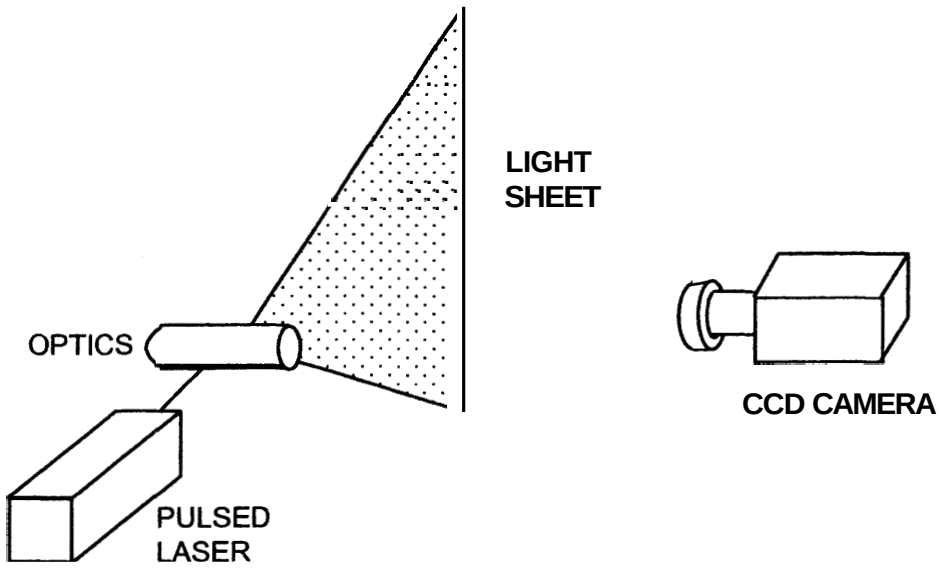

Figure 1. Schematic diagram illustrating the particle image velocimetry (PIV) technique.

Phase Doppler Interferometry (PDI)

Figure 2 presents a schematic diagram illustrating the PDT measurement method. PDI, which is an extension of laser Doppler velocimetry, utilizes intersecting laser beams to produce a fringe pattern where the beams intersect. When a drop passes through the fringe pattern (measurement volume), the scattered light has a frequency shift corresponding to the velocity of the drop (Doppler shift). By collecting the scattered light with multiple photo-detectors, the size and the velocity of the drop can be determined.

The PDI measurements were conducted in a sprinkler characterization facility in the Building and Fire Research Laboratory at NIST. The facility consists of an enclosed area equipped with the necessary piping and pumps to operate under a variety of flow conditions. The water is collected and recirculated back to the sprinkler, forming a closed

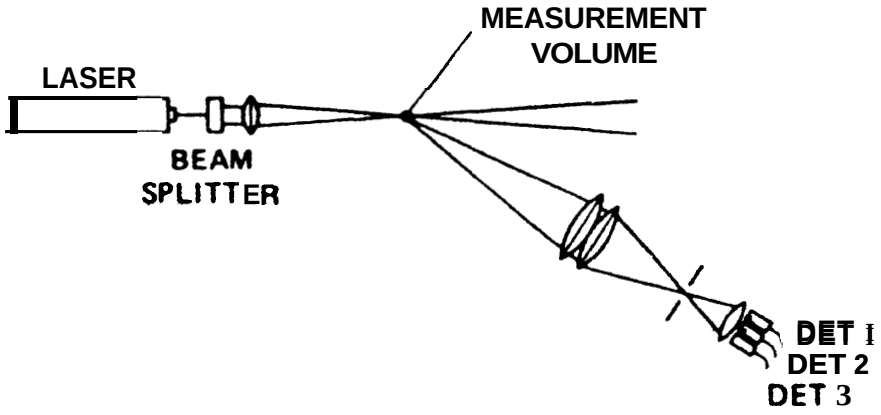

Figure 2. Schematic diagram illustrating the phase Doppler interferometry (PDI) technique.

loop system. The total dimensions of the enclosed pool used to collect the water spray is 6 m x 6 m, and the sprinkler can be mounted at one of several ports 1.6 m above the floor. **A** variety of diagnostics are being investigated for use in the facility to characterize water sprays.

The measurements presented here correspond to the spray generated with a Reliable Model GFR QR 701A fire sprinkler with a K-factor of 1.35×10^{-4} $m^3 s^{-1} kPa^{-0.5}$ (5.6 gal min^{-1} $psig^{-0.5}$). The pressure at the sprinkler head was maintained at 131.0 kPa ± 6.9 kPa (19 psig ± 1 psig), resulting in a flow rate through the sprinkler of 1.54×10^{-3} m^3 s^{-1} ± 0.051×10^{-3} m^3 s^{-1} (24.4 gpm ± 0.8 gpm). The sprays produced by fire sprinklers are large compared to systems in which PDI is typically applied, and cover an area on the order of 10 m^2. Due to the large coverage area, it is necessary to locate the PDI transmitting and receiving optics directly in the spray. This was accomplished by encasing both the transmitting and receiving optical systems in water-tight containers equipped with a purge of dry air to prevent moisture from condensing on the optics. The PDI optics are mounted on a rectangular translation stage that can be moved in either horizontal direction. The measurements were obtained in a horizontal plane 1.12 m ± 0.01 m below the sprinkler.

The experiments were conducted using a 2-component phase Doppler interferometer with a Real-time Signal Analyzer (RSA) available from TSI, Inc. **A** 300 mW air-cooled argon ion laser operating in multi-line mode was used as the illumination source, and the green (λ = 514.5 nm) and blue (λ = 488 nm) lines were used to measure the axial and radial velocity components, respectively. The transmitting optics were coupled to the beam conditioning optics using fiber optic cables, which permitted the transmitting optics to be located in the spray. The front lens on the transmitting optics had a focal length of 1000 mm, and a 50 mm extender (set of collimating lenses to change the laser beam intersection angle) was used to increase the maximum measurable drop size to 950 μm. The receiving optics were located at a scattering angle of 33° ± 1° measured from the direction of propagation of the laser beams.

The PDI signal processor was initially operated with the recommended settings for the flow investigated, although it was found that the system operated more effectively under other settings. This was due to burst splitting events that caused the processor to over-count drops, and is discussed below. The recommended operating conditions for the drop velocities under investigation here correspond to a sample frequency of 40 MHz (the rate at which the Doppler signal is sampled), mixer frequency of 36 MHz (mixers are used to reduce the signal frequency prior to analog-to-digital conversion), and a low pass filter setting of 20 MHz (low pass filters are used to remove the summed components from the downmixed signal, so that only the difference is used). The settings result from optimizing the processor for the expected Doppler frequency which is governed by the drop velocity and fringe spacing. The actual processor settings used when collecting the data presented in this paper were: mixer frequency = 40 MHz, sample frequency = 10 MHz, low pass filter = 1.25 MHz. Additional details of the experimental arrangement are available elsewhere [14. 17].

Results and Discussion

PDZ Measurements

Figure 3 presents representative size distributions collected at two locations in the spray. In each case, three size distributions, corresponding to replicated measurements at the same location, are shown to demonstrate the variability in the runs. The size distributions presented in Figures 3A and 3B correspond to data collected close to ($r < 0.5$ m) and far from ($r > 1.5$ m) the sprinkler axis, respectively. In general, data collected close to the sprinkler produced size distributions represented reasonably well by a log-normal model. Data obtained farther from the sprinkler, which are more heavily weighted by larger drops, produced size distributions more accurately modeled by Rosin–Rammler [18] size

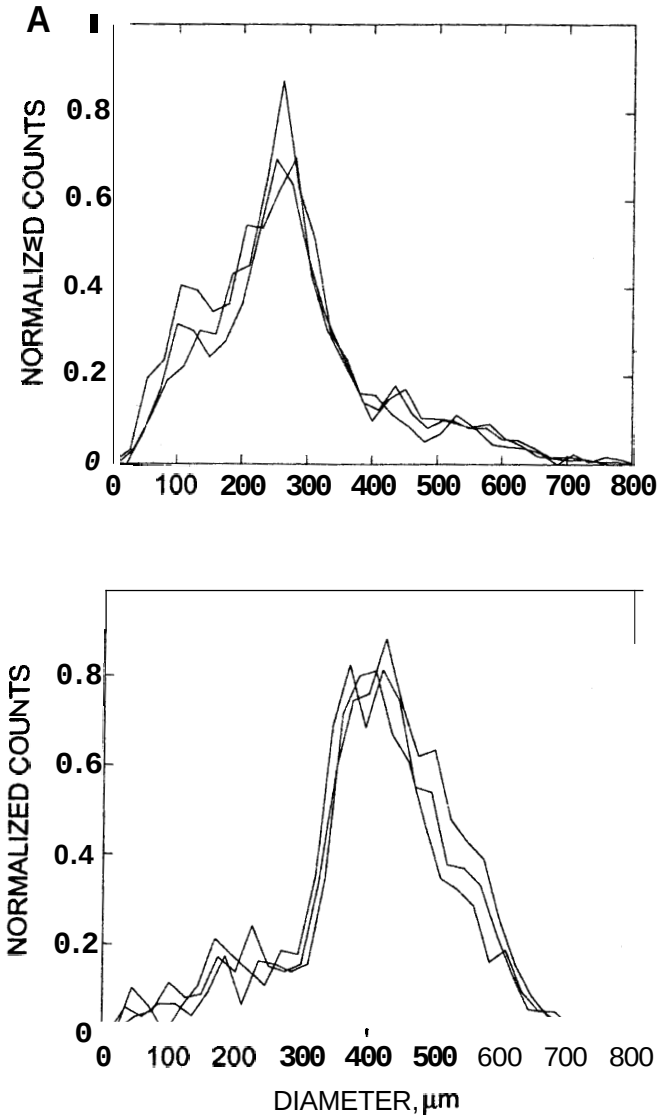

Figure 3. Representative size distributions obtained with the PDI system at locations (A) near ($r < 0.5$ m) and (B) far from ($r > 1.5$ m) the (Reliable) fire sprinkler axis. Maximum measurable drop diameter is limited by the optical system to 980 μm.

distributions. You [8] reported that measured size distributions were best represented by a modified size distribution model in which the smaller drops were represented by a log-normal distribution and the larger drops were represented by a Rosin–Ramrnler model. Current efforts at NIST include representing size distributions at all locations in the spray as a weighted mixture of log-normal and Rosin–Rammler distributions. Such a size distribution model could easily be incorporated into computational models intended to predict the interaction of fires and the water sprays produced by the experimentally characterized sprinklers.

Radial profiles of the arithmetic mean diameter (D_{10}), volume mean diameter (D_{30}), and Sauter mean diameter (D_{32}) are shown in Figure 4. Here the customary notation of Mugele and Evans is used [19], which corresponds to the accepted engineering definitions and not the statistical definitions based upon moments. The profiles represent data averaged over various angular coordinates, θ. The spray data presented correspond to 370 samples collected at 120 locations in a horizontal plane 1.12 m $\pm$ 0.01 m below the sprinkler head. A sample consisted of 2000 drop attempts (drops passing through the probe volume). The actual number of drops measured was less than this because not all signals were validated. Collecting larger sample sizes was impractical because of the low data rates associated with this low number density spray. Data rates typically varied from 0.1 Hz to 10 Hz. The measured values of D_{10}, D_{30}, and $D_{,,}$ were not found to vary significantly with the angular coordinate, but increased with increasing radial coordinate as shown in the figure. The arithmetic mean diameter, D_{10}, varied from approximately 200 μm where the size distributions were heavily weighted by the smaller drops to over 500 μm in the outer region of the spray. For large values of the radial coordinate, r, the size distributions are dominated by larger drops because the smaller drops have insufficient initial momentum to reach the outer spray region. The error bars in Figures 4–7

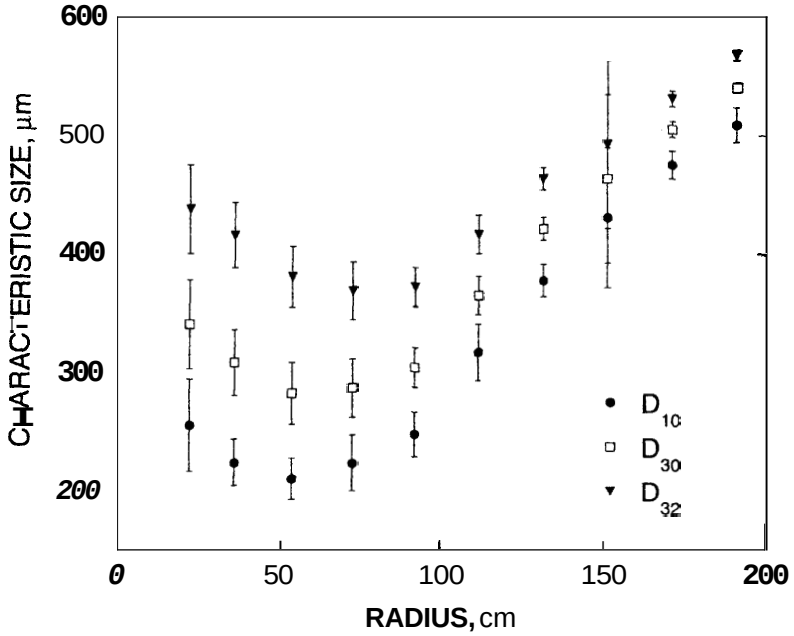

Figure 4. The arithmetic mean diameter (D_{10}), volume mean diameter (D_{30}), and Sauter mean diameter (D_{32}) as a function of the radial coordinate in the spray produced by the Reliable fire sprinkler.

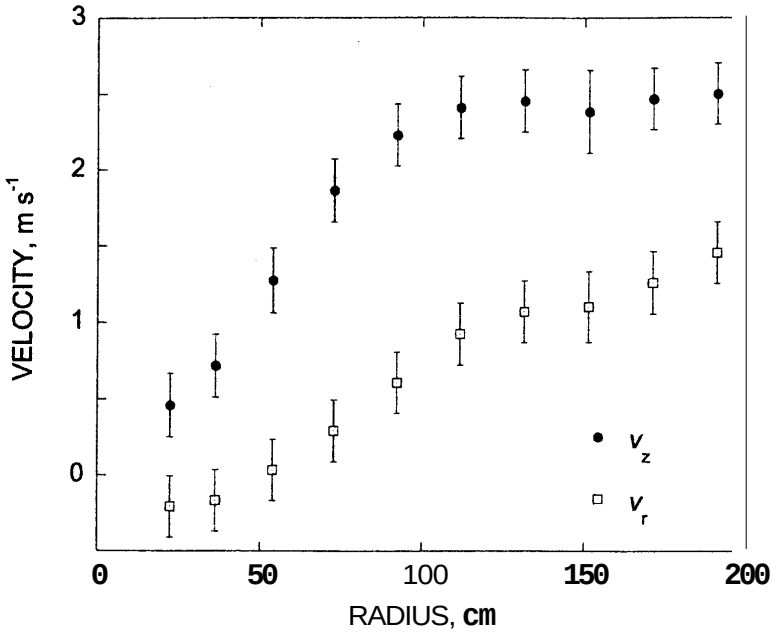

Figure 5. The mean axial (v_z) and radial (v_r) drop velocities measured in the spray produced by the Reliable fire sprinkler as a function of the radial coordinate.

correspond to a combined standard uncertainty with a coverage factor of $k = 2$, or roughly a 95% confidence interval [15, 16]. The quantification of the measurement uncertainty is discussed elsewhere [14].

Mean values of the axial (positive values correspond to downward) and radial drop velocities are presented as a function of the radial coordinate in Figure 5. As in Figure 4,

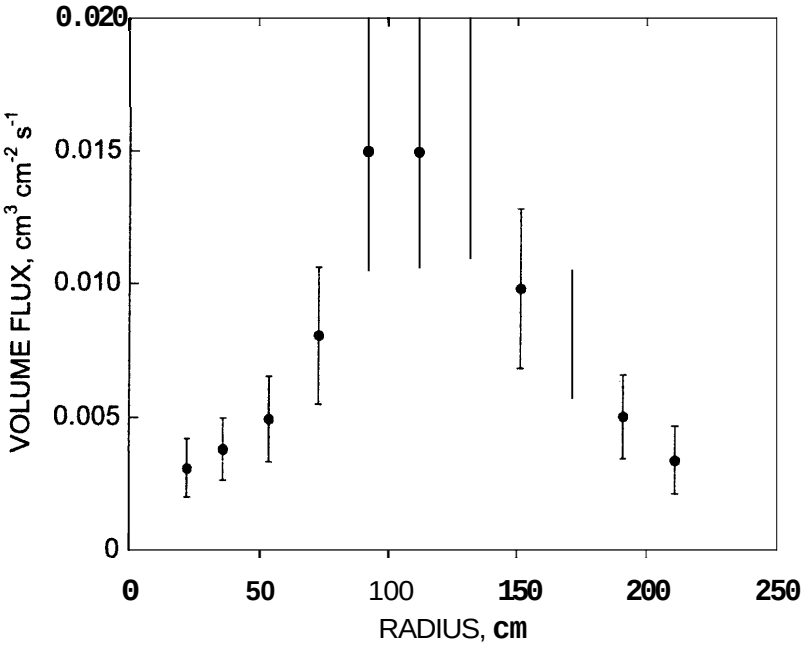

Figure 6. The volume flux measured with the PDI system as a function of the radial coordinate (Reliable fire sprinkler).

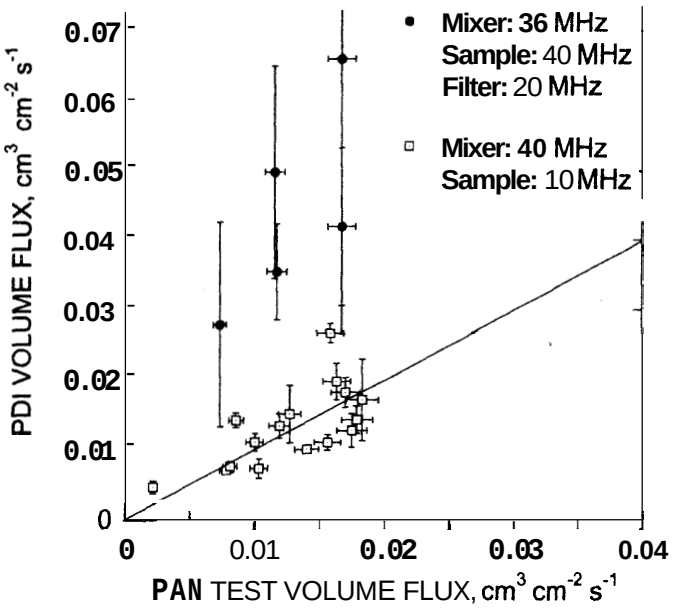

Figure 7. Comparison of the volume flux measured with the PDI system and the pan test measurements.

the data have been averaged over the angular coordinate. The drop velocities, like the characteristic sizes shown in Figure 4, were not found to vary significantly with the angular coordinate. The mean axial velocity is relatively low near the sprinkler axis (inner region of the spray), but increases with the radial coordinate until a maximum value of approximately 2.5 m s^{-1} at $r = 100$ cm is reached. The radial coordinate at which the mean axial velocity reaches a plateau corresponds to the location where the characteristic sizes begin to increase with r. The mean radial component of the drop velocity ranges from roughly -0.25 m s^{-1} to 1.5 m s^{-1}, and also increases with radial coordinate. In the inner region of the spray, negative radial velocities indicate a recirculation zone produced by the momentum transfer between the spray and the ambient gas, which is discussed further below.

Volume flux measurements presented in Figure 6 reveal that most of the water spray at a horizontal plane 1.12 m below the sprinkler flows through an annular ring approximately 0.5 m wide and centered at $r \approx 1.2$ m. The angular variation in the volume flux measurements was greater than the size or velocity measurements, which is attributable to the presence of the yoke arms that hold the deflector plate in place, the grooves on the deflector plate, and the inherent uncertainty in PDI volume **flux** measurements. The volume flux of drops crossing the PDI probe volume is calculated from the measured volume mean diameter (D_{30}), number density, and cross-sectional area of the probe volume. All of these quantities have associated uncertainties, and the propagation of these uncertainties make accurate volume **flux** measurements difficult to obtain with the PDI technique. Note that the dominant source of uncertainty in the volume flux calculation is the accurate determination of the probe area dimensions. The probe area, which is determined *in situ* during the measurements, depends upon the optical set-up and operating parameters of the PDI system (e.g., laser power, PMT detector gain), the size distribution

of the drops, and the accuracy to which the velocity and transit time of the drops can be determined.

The volume flux measurements display greater variation with respect to the angular coordinate than the size and velocity measurements; however, there is no obvious dependency on θ. This may be due to the randomness of the spray or insufficient measurement resolution. Although PDI is capable of measurements with fine resolution (<1 mm), the large coverage area of the sprinkler spray makes such measurements impractical. This is the primary disadvantage of using PDI in very large sprays like the one investigated here. Regardless of the cause, averaging over the angular coordinate, and including the angular variations in the Type **A** uncertainties **as** was done in Figure 6, results in useful volume flux profiles with reasonable measurement uncertainties, appropriate for use in fire dynamics models.

The volume flux profile shown in Figure 6 can be integrated over the radial coordinate to obtain a flow rate through the measurement plane, which can be compared with the flow rate of water through the sprinkler. The volumetric flow rate, V, through the sprinkler can be determined from the K-factor [20] and the pressure at the sprinkler head using the relation

$$V = KP^{0.5}, \tag{1}$$

where K is the numerical K-factor in the appropriate units and P is the water pressure (gauge) at the sprinkler head. Applying Equation (1) for the conditions used here, $V = 1.54 \times 10^{-3}\ \mathrm{m^3 s^{-1}} \pm 0.051 \times 10^{-3}\ \mathrm{m^3 s^{-1}}$. Integration of the volume **flux** profile in Figure 6 results in a flow rate through the measurement plane of $1.43 \times 10^{-3}\ \mathrm{m^3 s^{-1}} \pm 0.145 \times 10^{-3}\ \mathrm{m^3\ s^{-1}}$. Therefore, the integrated flow rate agrees with the value calculated from the sprinkler K-factor to within 8%, indicating that the volume flux profiles presented in Figure 6 are consistent with the total flow of water through the sprinkler head.

Doppler Burst Splitting

Figure 7 presents a comparison between the volume **flux** measurements obtained with the PDI system and pan test measurements in which the **flux** was measured using a graduated cylinder and a stopwatch. Note that although the measurement area for the pan tests ($31.4\ \mathrm{cm^2} \pm 1.0\ \mathrm{cm^2}$) is considerably larger than that of the PDI measurements (of order $0.01\ \mathrm{cm^2}$), it is orders of magnitude smaller than the area of the spray (approximately $10\ \mathrm{m^2}$). Because the characteristics of the spray do not vary significantly over the dimensions of the pan test measurement area, the fluxes determined from the pan tests can be compared directly with those obtained from the PDI measurements.

The filled symbols in Figure 7 correspond to measurements taken using the recommended PDI operating conditions. It is evident that the volume flux measured with the PDI system is considerably higher than the volume **flux** obtained from the pan test measurements, and also that there is considerable variation in the measurements. The vertical error bars represent only the Type **A** uncertainties ***(2s)***. The horizontal error bars represent the 6.6% combined standard uncertainty, $2U_c$, of the pan test measurements.

The PDI volume flux measurements are significantly higher than the actual flux due to the occurrence of burst splitting events. To measure the large drops present in this spray,

it is necessary to use a lens with a large focal length on the transmitting optics. This provides the increased fringe spacing necessary to size large drops. Because the coverage area of the spray and the distance between the transmitting optics and the probe volume are both large, the probability is high that drops will pass through the transmitting laser beams while another drop is in the sample volume. The result of drops attenuating the transmitting beams is a momentary loss of the fringe pattern. The processor improperly interprets this as the drop leaving the sample volume, and when the fringe pattern reappears, it is interpreted as another drop entering the sample volume. The result is that single drops are erroneously counted as multiple drops. Furthermore, the transit time of the drop is calculated incorrectly, which affects the calculation of the probe area. Thus, the burst splitting events have a significant impact on the data, particularly the volume flux and number density measurements [21].

The open symbols in Figure 7 correspond to PDI volume flux measurements obtained with the operating conditions optimized to minimize the effect of burst splitting. Note the much better agreement between the PDI volume flux measurements and the pan test measurements. To minimize the effect that burst splitting events have on the measurement, the sample frequency was reduced from 40 MHz to 10 MHz. This is the lowest value of the sample frequency used because attempts to calibrate the detector phase shifts at lower frequencies were unsuccessful. The cause of the unsuccessful calibrations is unknown and is under investigation.

The reason that the impact of the burst splitting events on the measurements is minimized by lowering the sampling rate is related to the discreteness of the sampling process used during PDI measurements. Reducing the sampling frequency has a beneficial effect on the measurements because the periods of low intensity that cause the bursts to be split are short-lived. By reducing the sampling rate, the probability that the processor will sample through the splitting event without detecting the brief periods of low signal intensity (below the signal threshold) is increased. **As** a result, the processor does not "close" the gate, which would falsely indicate that the drop has left the probe volume. Furthermore, the signal-to-noise ratio (SNR) is used to detect the presence of drops in the probe volume, and the SNR is increased by reducing the sample rate and the low pass filter, which further reduces the likelihood of burst splitting. The impact of burst splitting events on the data has been extensively investigated, and those results are presented elsewhere [21].

PIV Measurements

Figure 8 presents an image obtained during PIV measurements in the vicinity of a fire sprinkler. The calculated velocity vectors have been superimposed upon the image and show the initial mean velocity of the drops leaving the sprinkler. The data presented in Figure **8** are ideally suited to provide initial conditions for fire dynamics models such as FDS that predict the interaction of fire sprinklers with enclosure fires.

The velocity field (vector map) presented in Figure 8 was obtained from a PIV image pair by dividing the 1000 pixel x 1000 pixel images into 169 square interrogation regions. The vectors shown in Figure 8 correspond to the mean velocity in the corresponding interrogation regions. The interrogation regions are 77 pixels x 77 pixels in size, and therefore the resolution of the velocity measurement is 22.7 mm (77 pixels x 0.295 mm/pixel). The resolution can be increased by increasing the magnification of

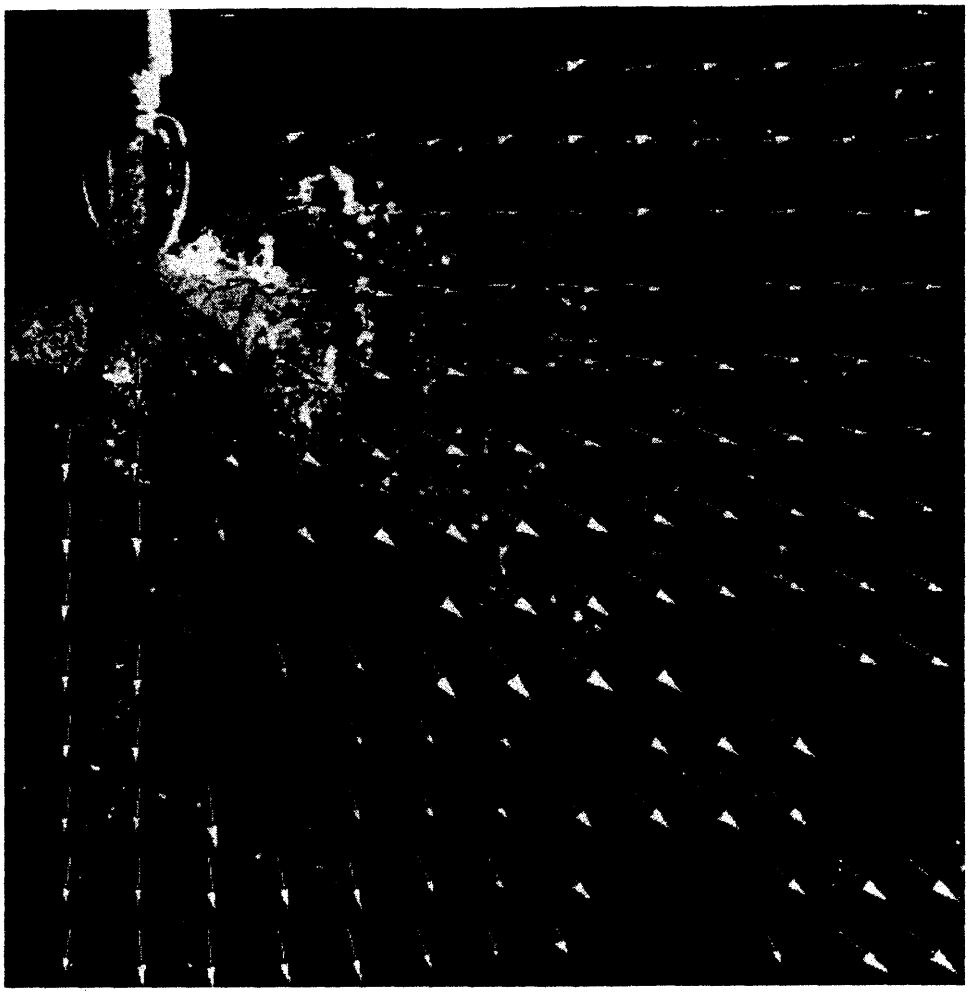

Figure 8. PIV measurements near the head of the Grinnel fire sprinkler.

the image; however, a balance must be achieved between the desire to capture a large planar image and increased resolution. The resolution used here represents an effective compromise between these competing objectives. Furthermore, care must be taken not to decrease the spatial resolution to the point that a large number of interrogation regions are void of drops. When PIV images are processed in which some of the interrogation regions do not contain any drops, the cross-correlation algorithm will correlate the noise in the two images, resulting in erroneous data. Interrogation regions in Figure 8 that do not contain vectors correspond to regions where the PIV processor performed cross-correlations on the noise in the images. To correct for vectors resulting from cross-correlations on the noise, 100 image pairs were obtained at each location and velocity vectors with lengths that deviated from the mean in that particular interrogation region by more than 3 standard deviations were removed from the data set [12]. Note that the velocity field presented in Figure 8 corresponds to a single image pair.

Figure 9 presents the measured "initial" values of the drop velocity determined from the PIV data. In this figure, the radial velocity corresponds to **a** spherical coordinate system in which the origin is located between the orifice and the deflector plate of the sprinkler. The location of the origin was determined by extrapolating the measured

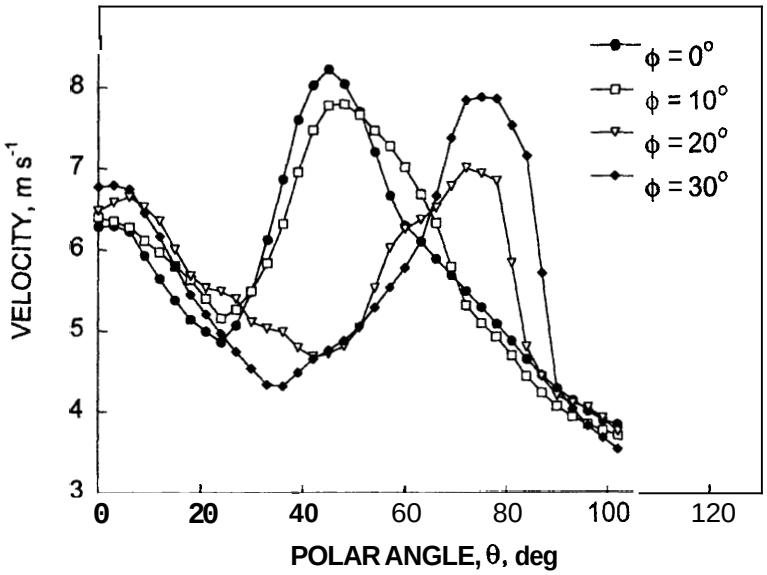

Figure 9. Radial velocity of water drops (spherical coordinates) 200 mm from the (Grinnel) sprinkler.

velocity vectors (such as those presented in Figure 8) backward to a common point. The abscissa in Figure 9 corresponds to the polar angle, 8, as measured from a vertical line from the sprinkler to the floor. The azimuthal coordinate, ϕ, is measured from one of the sprinkler yoke arms. Note that the sprinkler has four planes of symmetry; thus, accurately characterizing the spray in one quadrant adequately describes the sprinkler spray. The data presented in Figure 9 correspond to radial velocities 200 mm from the origin determined by linear interpolation.

The data presented in Figure 9 indicate that there is variation in the drop velocities with both the polar and azimuthal angles. The velocity profiles corresponding to $\phi = 0$" and $\phi = 10$" display peaks near $\theta = 45°$, with peak velocities of approximately 8 m s^{-1}. The velocity profiles corresponding to azimuthal angles of $\phi = 20$" and $\phi = 30$" peak near $8 = 75°$, with peak velocities of 7 m s^{-1} and 8 m s^{-1}, respectively. This variation **is** attributed to the presence of the yoke arms and the grooves in the deflector plate.

Using the data presented in Figure 9 as initial conditions, the volume flux of water on the floor was predicted using a simple drop trajectory model [12]. The model, which is comprised of a momentum balance between the acceleration due to gravity and the drag on the drop, also requires knowledge of the initial flux distribution of water leaving the sprinkler. This was approximated from the PIV images by considering the spatial distribution of drops in the images. It was assumed that the volume of water in the measurement volume correlates with the area (pixel density) imaged. **A** threshold value of the gray-scale image intensity was chosen such that the drops could be distinguished from the background, and the fraction of pixels corresponding to imaged drops was determined as a function of the polar and azimuthal angles. Only regions of the images corresponding to **a** radial distance of 200 mm $\pm$ 25 mm were included in the calculations, which corresponds to the location where the drops could be distinguished from the ligaments that initially extend from the sprinkler. The relative drop density was averaged over 3" increments of the polar angle ($\Delta\theta = 3°$) for each of the azimuthal angles presented in

Figure 9. The water flux was calculated by normalizing the relative drop density obtained using the above procedure by the flow rate through the sprinkler head, and is presented in Figure 10.

Several assumptions used in the model should be noted. First, the drop size distribution leaving the sprinkler is unknown; therefore, the drop sizes were assumed to obey a Rosin-Rammler distribution [18] with an identical mean diameter and distribution function for all angles. The feasibility of using phase Doppler interferometry to measure the drop size distributions close to the sprinkler head is under investigation. Difficulties exist when attempting to apply this diagnostic technique in very dense regions of sprays [e.g., 22]. The model also assumes that the spray has uniform characteristics in the azimuthal direction in the range $30" \leq \phi \leq 90°$. Variations of the spray characteristics have also been averaged over 10" increments in the polar direction. Furthermore, the influence of the spray on the surrounding air has been neglected, and drop-drop interactions have been ignored. Lastly, the drag force on the drops was calculated using laminar flow and hard-sphere approximations [23]. Note that assuming **a** drop velocity of 8 m s^{-1} results in a calculated Reynolds number of 530 for a drop with a diameter of 1 mm. Thus, the laminar flow assumption is reasonable, although the hard-sphere approximation may result in the drag force being overpredicted.

Figure 11 presents a comparison of the predicted water flux on the floor beneath the sprinkler and the water flux determined from pan test measurements. The pan tests presented in Figure 11 correspond to water collected in rectangular pans (30.5 cm x 30.5 cm) located **3** m beneath the sprinkler. The data, which have been averaged over the azimuthal coordinate, indicate good agreement between the measured and predicted volume flux. Thus, the PIV measurements described here, combined with the flow rate through the sprinkler, can be used to provide needed volume flux data for the fire dynamics simulations. Note that the data presented in Figures 6 and 11 do not correspond to the

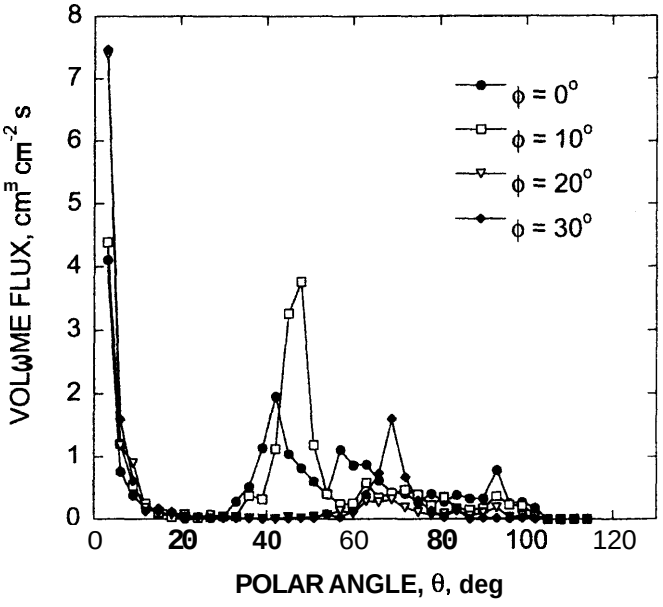

Figure 10. Calculated volume flux of water drops leaving the (Grinnel) sprinkler.

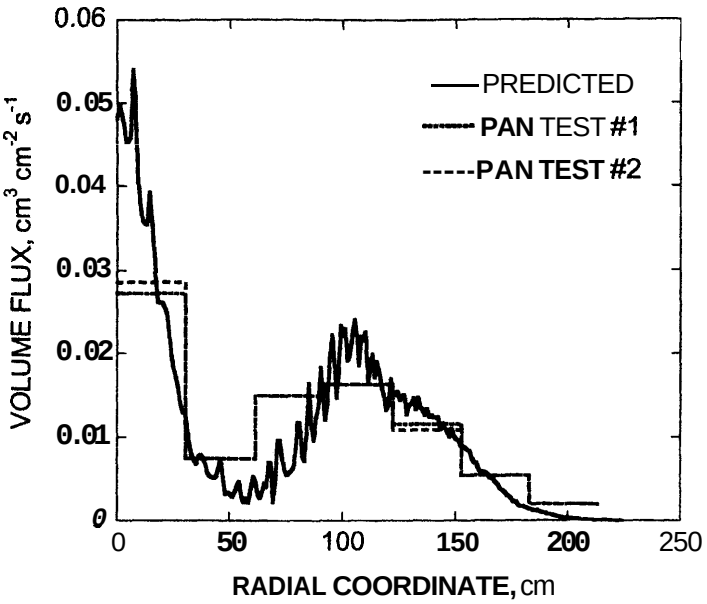

Figure 11. Radial profiles of the measured and predicted volume flux of water on the floor (3 m below the Grinnel fire sprinkler).

same spray, and therefore the volume flux profiles are considerably different. The peak near the sprinkler axis in the volume flux profile in Figure 11 results from a combination of the sprinkler design and the low water pressure used to generate this spray. The data in Figure 6, which correspond to different sprinkler operating at higher water pressure, does not display this peak in the volume flux profile near the sprinkler axis.

It should be noted that the pixel density corresponding to drops described above scales with the diameter of the drops to the second power (d^2), whereas the volume **flux** scales with the diameter of the drops to the third power (d^3). Furthermore, the near-instantaneous images produced during the PIV measurement corresponds to a spatial measurement, whereas accurate volume flux measurements require a temporal measurement. Temporal measurements, which correspond to measuring drops passing through a sampling cross section, include collection techniques (e.g., pan tests) and optical instruments that sense individual drops (e.g., PDI). If all of the drops have the same velocity, then the spatial and temporal distributions will be identical. However, it is known that this is not the case in fire sprinkler sprays or other sprays of practical interest [17]. Thus, although the data presented here show good agreement between the PIV measurements combined with the trajectory model and the pan test measurements, additional research is required to determine over what range of drop sizes, drop velocities, and water flow rates this method is reliable.

A comparison of the axial velocity determined from the PIV measurements and the PDI measurements at 1.12 m below the sprinkler head is shown in Figure 12. The volume flux profile determined from the PDI data is shown for comparison. The data in Figure 12, which correspond to measurements obtained in the spray produced by the Reliable fire sprinkler, show good agreement between the two diagnostic techniques in the core region of the spray ($r \approx 1.0$ m). Near the sprinkler axis (small values of the radial coordinate) there is discrepancy between the two measurements. The mean velocity obtained from the PDI measurements is considerably lower than that obtained

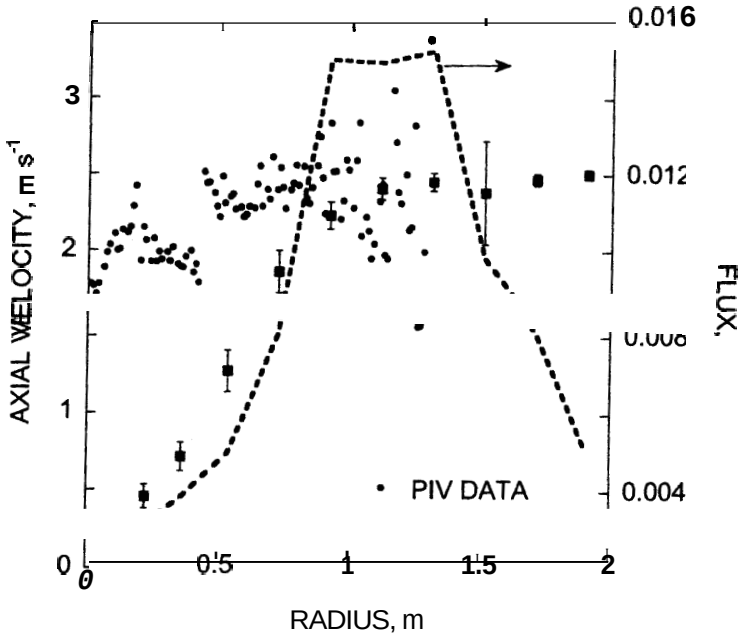

Figure 12. Comparison of **PIV** and **PDI** axial velocity measurements. The volume flux of water drops obtained from the PDI measurements is shown for comparison. The data correspond to the spray produced by the Reliable fire sprinkler with the same operating conditions as Figures 4-6.

from the PIV measurements. This is attributed to several factors. First, the PDI data is heavily weighted by the many smaller drops present in this region of the spray (see Figure 3). Because there are strong size velocity correlations present in the spray, the PDT measurements are weighted towards these lower velocities [17]. Also, PDI measurements conducted in the NIST facility were obtained at a height approximately 0.5 m above the floor, which resulted in the velocity measurements being affected by recirculation regions in the experimental facility. This is shown pictorially in Figure 13, and discussed further in [17]. The velocity of the surrounding air may have had the opposite effect on the PIV measurements because that data were obtained at a much higher elevation in the UL sprinkler facility. In that case, the recirculation zone along the sprinkler axis may not extend to the measurement elevation, or may not exist in the interior of the spray at all.

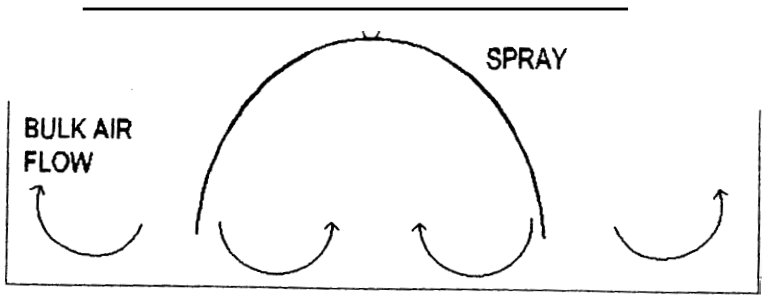

Figure 13. Bulk air movement in the NIST sprinkler facility during the sprinkler characterization experiments.

Simulations are being conducted using FDS to gain further insight into the nature of the ambient air movement in the sprinkler facility.

Another factor that may contribute to the discrepancy observed is the very broad size distribution of the drops. In conventional PIV measurements, velocity fields are determined by correlating the displacement of two particle images corresponding to a small time difference. This is accomplished by introducing seed particles with a narrow size distribution (typically 1–3 μm) to the fluid, and assuming that the particles follow the fluid flow and thus act as "tracers" or "scatterers." In the application of PIV to **fire** sprinkler sprays, the water drops, which can vary in size from less than 10 μm to over 1000 μm, act as the tracer particles. The influence of using scatterers of such a broad size distribution has not been previously investigated. Furthermore, the intensity of light scattered by the drops scales as the square of the drop diameter (d^2). Thus, a 100 : 1 range in drop size results in a 10,000 : 1 dynamic range in light scattering intensities, which far exceeds the capabilities of the CCD arrays used in PIV measurements. Investigations of the influence of a very broad range in particle size or light scattering intensity on PIV measurements has not been previously reported in the literature. This is **a** measurement issue requiring further investigation.

Despite the discrepancy in the axial velocity measurements for values of the radial coordinate below 0.7 m shown in Figure 12, the measurements are in good agreement for the majority of the spray. That is, numerical integration of the volume **flux** profile reveals that the region of the spray in which the two velocity measurements differ by more than 25% ($r \leq 0.7$ m) constitutes only 7% of the total water flow. Thus, on **a** volume basis, the agreement between the PIV and PDI velocity measurements is good for most of the water spray, and the discrepancy is limited to the region of small drops along the sprinkler axis.

For large values of the radial coordinate ($r \geq 1.2$ m) PIV measurements are increasingly difficult due to the low number density of drops in this region of the spray. In the dilute regions of the spray, particle tracking velocimetry (PTV) may be a more appropriate technique. In PTV, the displacement **of** individual drops is determined from the image pairs instead of utilizing cross-correlation algorithms. The complimentary technique, PDI, results in reliable measurements for large values of the radial coordinate; however, long data acquisition times are required. In addition, the mean velocities obtained from PDI measurements may be affected by small droplets that are entrained in recirculation zones, as discussed above.

Conclusion

It has been demonstrated that phase Doppler interferometry (PDI) and particle image velocimetry (PIV) permit accurate and non-intrusive characterization of fire sprinkler sprays. PIV has the advantages that it is a planar imaging technique and that data can be obtained very rapidly. Unfortunately, PIV measures only the mean drop velocity, and no information is obtained on the drop size distribution. The complimentary technique, PDI, provides data on both the drop size and velocity; however, obtaining information throughout a spray can be a tedious process due to the small measurement volume and low data rates typical of fire sprinkler sprays. Together these two diagnostic methods can

provide the measurements required to include fire sprinklers in **FDS** and other computer models.

cknowledge

The authors would like to thank Cary Presser for the **use** of the PDI system. Also, the contributions of Jacob Goodman and Daniel Landau were invaluable during **the** PDI measurements. Two of the authors (DTS, RML) would like to acknowledge the financial support of the **NIST** Fire Research Grants Program.

Notes

1. Current affiliation: Fire Research Laboratory, Bureau of Alcohol, Tobacco and Firearms, Rockville, MD 20850
2. Unless otherwise stated, all uncertainties reported herein correspond to the combined standard uncertainty, U_c, with a coverage factor, $k = 2$ (i.e., $2U_c$) [15, 16].
3. Certain commercial equipment, materials, or software are identified in this manuscript to specify adequately the experimental procedure. Such identification does not imply recommendation or endorsement by the National Institute of Standards and Technology, nor does it imply that the materials or equipment are necessary the best available for this purpose.

References

[1] G. Grant, J. Brenton, and D. Drysdale, "Fire Suppression by Water Sprays," *Progress in Energy and Combustion Science,* vol. 26, 2000, pp. 79–130.

[2] H.R. Baum, K.B. McGrattan, and R.G. Rehm, "Three Dimensional Simulations of Fire Plume Dynamics," *Journal of the Heat Transfer Society of Japan*, vol. *35,* 1997, pp. 45–52.

[3] K.B. McGrattan, H.R. Baum, and R.G. Rehrn, "Large Eddy Simulations of Smoke Movement," *Fire Safety Journal,* vol 30, 1998, pp. 161–178.

[4] J.R. Lawson, W.D. Walton, and D.D. Evans, "Measurement of Droplet Size in Sprinkler Sprays," National Bureau of Standards, **U.S.** Department of Commerce, NBSIR 88-3715, Gaithersburg, MD, February 1988.

[5] P.F. Nolan, "Feasibility Study of Using Laser High Speed Cine Systems for the Characterization of Droplets from Sprinkler Sprays," The Swedish Fire Research Board, Stockholm, Sweden, 1989.

[6] L.A. Jackman, P.F. Nolan, and H.P. Morgan, "Characterization of Water Drops from Sprinkler Sprays,'' *Fire Suppression Research–First International Conference,* Stockholm, Sweden, 1992, pp. 159–184.

[7] W.K. Chow, and L.C. **Shek,** "Physical Properties of a Sprinkler Water Spray," *Fire and Materials,* vol. 17, 1993, **pp.** 279–292.

[8] H.Z. You, "Sprinkler Drop-Size Measurement, Part 11: An Investigation of the Spray Patterns of Selected Commercial Sprinklers with the FMRC PMS Droplet Measuring System," Technical Report 0G1e7.RA 070(A), Norwood, **MA,** May 1983.

[9] H.Z. You, "Investigation of Spray Patterns of Selected Sprinklers with the FMRC Drop Size Measuring System," *Fire Safety Science—Proceedings of the First International Symposium,* Gaithersburg, MD, October 1985, pp. 1165–1176.

[10] T.S. Chan, "Measurements of Water Density and Drop Size Distributions of Selected ESFR Sprinklers," *Journal of Fire Protection Engineering,* vol. *6,* 1994, **pp.** 79–87.

[11] A.D. Putorti, T.D. Belsinger, and W.H. Twilley, "Determination of Water Spray Drop Size and Speed from a Standard Orifice, Pendent Spray Sprinkler," Report of Test. National Institute of Standards and Technology, Gaithersburg, MD, May 1999.

[12] D.T. Sheppard, P.D. Gandhi, and R.M. Lueptow, "Predicting Sprinkler Water Distribution Using Particle Image Velocimetry," *Proceedings Fire Suppression and Detection Research Application Symposium. Research and Practice: Bridging the* ***Gap.*** National Fire Protection Research Foundation, Orlando, **FL,** February 1999.

[13] P.D. Gandhi, and D. Steppan, "Using PDPA in Evaluation of Sprinklers," *Proceedings Fire Suppression and Detection Research Application Symposium. Research and Practice: Bridging the Gap*. National Fire Protection Research Foundation, Orlando, FL, February 1999, pp. 65–78.

[14] J.F. Widmann, "Characterization of a Residential Fire Sprinkler Using Phase Doppler Interferometry," *Atomization and Sprays,* vol. *36,* 2001, in press.

[15] B.N. Taylor, and C.E. Kuyatt, "Guidelines **for** Evaluating and Expressing the Uncertainty of NIST Measurement Results," NIST Technical Note 1297, National Institute of Standards and Technology, Gaithersburg. MD, September 1994.

[16] American National Standard for Expressing Uncertainty—U.S. Guide to the Expression of Uncertainty in Measurement. ANSI/NCSL Report Z540-2-1997, National Conference of Standards Laboratories, Boulder, CO, October 1997.

[17] J.F. Widmann, "Phase Doppler Interferometry Measurements in Water Sprays Produced by Residential Fire Sprinklers," *Fire Safety Journal,* vol. *36,* pp. 545–567, 2001.

[18] P. Rosin, and E. Rammler, "The Laws Governing the Fineness of Powdered Coal," *The Institute of Fuel,* October 1933, pp. 29–36.

[19] **R.A.** Mugele, and H.D. Evans, "Droplet Size Distribution in Sprays," *Industrial and Engineering Chemistry,* vol. 43, no. 6, 1951, pp. 1317–1324.

[20] R.P. Fleming, "Automatic Sprinkler System Calculations." In *The SFPE* ***Handbook*** *of Fire Protection Engineering,* 2nd ed., Quincy, MA: National Fire Protection Association, June 1995.

[21] J.F. Widmann, C. Presser, and S.D. Leigh, "Identifying Burst Splitting Events in Phase Doppler Interferometry Measurements," *Atomization and Sprays,* 2001, in press.

[22] W.D. Bachalo, R.C. Rudoff, **A.** Brena de la Rosa, "Mass Flux Measurements of a High Number Density Spray System Using the Phase Doppler Particle Analyzer," *AIAA 26th Aerospace Sciences Meeting and Exhibit,* Reno, NV, 1988, paper no. AIAA-88-0236.

[23] F.M. White, Viscous *Fluid Flow,* 2nd ed., New York: McGraw Hill, 1991.